The behaviour of materials under combined steady and oscillatory shear

1971 J. Phys. A: Gen. Phys. 4 85

(http://iopscience.iop.org/0022-3689/4/1/012)

J. Phys. A: Gen. Phys., 1971, Vol. 4. Printed in Great Britain

The behaviour of materials under combined steady and oscillatory shear

T. E. R. JONES and K. WALTERS

Department of Applied Mathematics, University College of Wales, Aberystwyth, Wales

MS. received 13*th July* 1970

Abstract. We consider the behaviour of elastico–viscous liquids as they deform under the action of an unsteady shear field consisting of a small-amplitude oscillatory shear superimposed on a steady simple shear. The theory for such a situation is developed in detail and certain predictions, some quantitative, and some qualitative, are made. These predictions are shown to be in good agreement with experimental results obtained from a Weissenberg rheogoniometer for certain aqueous polymer solutions.

1. Introduction

There is a growing interest in the flow behaviour of non-Newtonian liquids as they deform under the action of a combined steady and oscillatory shear (see, for example, Osaki *et al.*, 1965, Booij 1966 a,b, Macdonald and Bird 1966, Tanner 1968, Pipkin 1968). Although some attention has been paid to the case when the oscillatory shear is orthogonal to the steady shear (Tanner and Simmons 1967), most interest has been centred on the situation in which both the steady and the unsteady shear are in the same direction. For this second situation, any theoretical predictions can be immediately examined experimentally on a Weissenberg rheogoniometer, since this instrument has facilities for subjecting a material to a combined steady and oscillatory shear of the required sort.

Previous investigators have concentrated on the effect of the superimposed steady shear on the oscillatory motion. In particular, they have been concerned with the effect of the steady shear on the dynamic viscosity η' and dynamic rigidity G' measured as functions of the frequency of oscillation. We shall give some consideration to this aspect of the problem, but our primary concern will be the effect of the *oscillatory* shear on the *mean* motion. We will be concerned exclusively with the shear stress σ and no consideration will be given to the normal stresses.

In § 2 we develop the theory for superimposed flow in the cone-and-plate geometry. Certain predictions are made, some quantitative some qualitative, and these are checked experimentally in § 3.

2. Theory

We refer all physical quantities to spherical polar coordinates (r, θ, χ), the cone and plate being given by $\theta = \beta$ and $\theta = \pi/2$, respectively. The axis of rotation is taken as the polar axis and the appropriate velocity distribution is then $(0, 0, r \sin \theta w(\theta, t))$, where $r \sin \theta w$ is the physical component of the velocity in the χ direction. We have tacitly assumed that the gap between the cone and the plate is small and that inertial effects can be ignored, so that secondary flows are not relevant (cf. Oldroyd 1958, Walters 1962, 1968, Walters and Waters 1968).

The shear rate γ is given by

$$\gamma = \sin\theta \frac{\partial w}{\partial \theta}. \tag{1}$$

If the plate is given a forced motion consisting of a steady and an oscillatory part, and the cone is constrained by a torsion wire, the relevant form for γ in the liquid is

$$\gamma = q\{1 + \epsilon F(\theta)\exp(\mathrm{i}\omega t)\} \tag{2}$$

where

$$\epsilon = \frac{\alpha\omega}{q}. \tag{3}$$

In (2), F is a non-dimensional complex function of θ and the real part is implied. In (3), α is the angular amplitude and ω is the frequency of oscillation of the plate. We shall assume that ϵ is sufficiently small for terms of order ϵ^3 to be ignored.

For a small gap between the cone and the plate, the steady shear q is given by the constant value (cf. Walters and Waters 1968, Walters 1968)

$$q = \frac{\Omega}{(\pi/2 - \beta)} \tag{4}$$

where Ω is the (steady) angular velocity of the plate. Further, the function F is given by (cf. Walters and Kemp 1968)

$$F = \frac{\mathrm{i}\{\exp(\mathrm{i}c) - \mathscr{I}\}}{(\pi/2 - \beta)} \tag{5}$$

where $\mathscr{I}\alpha$ is the angular amplitude of the motion of the cone and c is the phase lag of the cone behind the plate. It is easily verified that (4) and (5) satisfy the equations of motion for any proposed equations of state.

We next need to consider suitable equations of state relating appropriate stress and deformation variables. For the deformation variable, we take (cf. Oldroyd 1950)

$$G_{ik} \equiv \frac{\partial x'^m}{\partial x^i}\frac{\partial x'^s}{\partial x^k} g_{ms}(\boldsymbol{x}') - g_{ik}(\boldsymbol{x}) \tag{6}$$

where g_{ik} is the metric tensor of a coordinate system x^i and x'^i is the position at time t' of the element that is instantaneously at the point x^i at time t.

If we write the displacement functions x'^i as r', θ', χ', it is easily verified that, for the velocity distribution under consideration,

$$\begin{aligned} r' &= r \\ \theta' &= \theta \\ \chi' &= \chi - \int_{t'}^{t} w(\theta, \tau)\,\mathrm{d}\tau. \end{aligned} \tag{7}$$

From (6) and (7), the physical components of G_{ik} can be shown to be

$$G_{(ik)} = \begin{pmatrix} 0 & 0 & 0 \\ 0 & D^2 & -D \\ 0 & -D & 0 \end{pmatrix} \tag{8}$$

where

$$D = \mathrm{Re}\left(q(t-t') - \mathrm{i}\frac{\epsilon}{\omega} qF \exp(\mathrm{i}\omega t)[1-\exp\{-\mathrm{i}\omega(t-t')\}]\right). \tag{9}$$

We shall be concerned only with the shear stress σ, which, on account of (8), can be written in the form (cf. Pipkin 1966)

$$\sigma(t) = F^{t}_{-\infty}\{D(t-t')\} \tag{10}$$

where F is a functional. We note from (8) and (9) that, provided ϵ is sufficiently small, the deformation is equivalent to a slight perturbation of a state of steady shear flow. The work of Pipkin (1966) implies, therefore, that (10) can be written in the simplified form

$$\sigma = \sigma_0 + \int_{-\infty}^{t} \varphi_1(q, t-t')\Delta D(t-t')\,\mathrm{d}t'$$
$$+ \int_{-\infty}^{t}\int_{-\infty}^{t} \varphi_2(q, t-t', t-t'')\Delta D(t-t')\Delta D(t-t'')\,\mathrm{d}t'\,\mathrm{d}t'' \tag{11}$$

where

$$\Delta D = -\mathrm{i}\frac{\epsilon}{\omega} qF \exp(\mathrm{i}\omega t)[1-\exp\{-\mathrm{i}\omega(t-t')\}] \tag{12}$$

and terms of order ϵ^3 have been ignored. In equation (11), σ_0 is the unperturbed shear stress given by

$$\sigma_0 = q\eta(q) \tag{13}$$

$\eta(q)$ being the shear-dependent apparent viscosity. φ_1 and φ_2 satisfy the consistency relations (cf. Pipkin 1966)

$$\int_0^\infty \varphi_1(q, \xi)\xi\,\mathrm{d}\xi = \frac{\mathrm{d}\sigma_0}{\mathrm{d}q} \tag{14}$$

$$\int_0^\infty\int_0^\infty \varphi_2(q, \xi_1, \xi_2)\xi_1\xi_2\,\mathrm{d}\xi_1\,\mathrm{d}\xi_2 = \frac{1}{2}\frac{\mathrm{d}^2\sigma_0}{\mathrm{d}q^2}. \tag{15}$$

Substituting (12) into (11) and making use of the result

$$\mathrm{Re}(f_1)\,\mathrm{Re}(f_2) = \tfrac{1}{2}\{\mathrm{Re}(f_1 f_2) + \mathrm{Re}(f_1\bar{f}_2)\} \tag{16}$$

where f_1 and f_2 are complex functions and the bar denotes the complex conjugate, we obtain

$$\sigma = \sigma_0 - \mathrm{i}\frac{\epsilon q}{\omega} F\exp(\mathrm{i}\omega t)\int_0^\infty \varphi_1(q, \xi)\{1-\exp(-\mathrm{i}\omega\xi)\}\,\mathrm{d}\xi$$
$$+ \frac{\epsilon^2 q^2 F\bar{F}}{2\omega^2}\int_0^\infty\int_0^\infty \varphi_2(q, \xi_1, \xi_2)\{1-\exp(-\mathrm{i}\omega\xi_1)\}\{1-\exp(\mathrm{i}\omega\xi_2)\}\,\mathrm{d}\xi_1\,\mathrm{d}\xi_2$$
$$- \frac{\epsilon^2 q^2 F^2\exp(2\mathrm{i}\omega t)}{2\omega^2}\int_0^\infty\int_0^\infty \varphi_2(q, \xi_1, \xi_2)\{1-\exp(-\mathrm{i}\omega\xi_1)\}$$
$$\times\{1-\exp(-\mathrm{i}\omega\xi_2)\}\,\mathrm{d}\xi_1\,\mathrm{d}\xi_2. \tag{17}$$

In the case of a small gap angle and negligible fluid inertia, the relevant stress equation of motion is

$$\frac{\mathrm{d}\sigma}{\mathrm{d}\theta} = 0. \tag{18}$$

It is easily verified that (17) with (4) and (5) satisfy this equation.

In the case of a small-amplitude oscillatory motion *without* any superimposed steady shear, it is customary to write (cf. Walters 1968)

$$\sigma = \eta^* \gamma \tag{19}$$

which from (2) becomes essentially

$$\sigma = \eta^* \epsilon q F \exp(\mathrm{i}\omega t). \tag{20}$$

η^* is called the complex viscosity and is usually written in the form

$$\eta^* = \eta' - \frac{\mathrm{i}G'}{\omega} \tag{21}$$

where η' is called the dynamic viscosity and G' the dynamic rigidity. We see from (17) that, in the case of superimposed steady shear, it is possible to define an effective complex viscosity given by

$$\eta^* = -\frac{\mathrm{i}}{\omega}\int_0^\infty \varphi_1(q, \xi)\{1 - \exp(-\mathrm{i}\omega\xi)\}\,\mathrm{d}\xi. \tag{22}$$

In the limiting case as $\omega \to 0$, (22) reduces to

$$\eta^*|_{\omega \to 0} = \int_0^\infty \varphi_1(q, \xi)\xi\,\mathrm{d}\xi = \frac{\mathrm{d}\sigma_0}{\mathrm{d}q} \tag{23}$$

which implies that

$$\left.\begin{aligned} &\eta' \to \frac{\mathrm{d}\sigma_0}{\mathrm{d}q} \quad \text{as} \quad \omega \to 0 \\ \text{and} \quad &G' \to 0 \quad \text{as} \quad \omega \to 0. \end{aligned}\right\} \tag{24}$$

This result was obtained by a different method in our previous work (Walters and Jones 1968) and was also derived at about the same time by Markovitz (1968) and Pipkin (1968).

Our primary concern in the present paper is the effect of the oscillation on the mean shear stress and the mean couple. From (17), we see that to order ϵ^2, the mean shear stress is given by

$$\sigma = \sigma_0 + \frac{\epsilon^2 q^2 F\bar{F}}{2\omega^2}\int_0^\infty\int_0^\infty \varphi_2(q, \xi_1, \xi_2)\{1 - \exp(-\mathrm{i}\omega\xi_1)\}\{1 - \exp(\mathrm{i}\omega\xi_2)\}\mathrm{d}\xi_1\,\mathrm{d}\xi_2 \tag{25}$$

where terms of order ϵ^4 have been ignored. From (25), it is easily deduced that the percentage decrease I in the mean couple on one of the instrument members is given by

$$I = -\frac{100\epsilon^2 q^2 F\bar{F}}{2\omega^2\sigma_0}\int_0^\infty\int_0^\infty \varphi_2(q, \xi_1, \xi_2)\{1 - \exp(-\mathrm{i}\omega\xi_1)\}\{1 - \exp(\mathrm{i}\omega\xi_2)\}\,\mathrm{d}\xi_1\,\mathrm{d}\xi_2 \tag{26}$$

where terms of order ϵ^4 have been ignored.

If $\omega \to 0$, with q fixed, it is easily verified that $I \to 0$. On the other hand, if $\omega \to 0$ with ϵ fixed, we see that

$$I|_{\omega \to 0} = -\frac{100\epsilon^2 q^2 F\bar{F}}{4\sigma_0}\frac{\mathrm{d}^2\sigma_0}{\mathrm{d}q^2}. \tag{27}$$

Equations (24) and (27) imply that in the limit of zero frequency all elastico-viscous liquids behave as a non-Newtonian *inelastic* liquid characterized only by its shear-dependent viscosity $\eta(q)$. The predictions embodied in equations (24) and (27) will be examined experimentally in § 3.

For general values of ω, it is not possible to make quantitative predictions at the present time, since it is not possible to specify the functions φ_1 and φ_2. However, qualitative predictions may be made by appealing to a simple fluid model. We take an Oldroyd (1958) model, since Booij (1966 a,b) has used such a model with some success in predicting the general shape of the dynamic viscosity and dynamic rigidity curves for non-zero q.

For equations of state of the form†

$$p_{ik} = -pg_{ik} + p_{ik}' \tag{28}$$

$$p'^{ik} + \lambda_1 \frac{\mathfrak{d}}{\mathfrak{d}t} p'^{ik} + \mu_0 p'^{j} e\{(1)ik\} = 2\eta_0\left(e\{(1)ik\} + \lambda_2 \frac{\mathfrak{d}}{\mathfrak{d}t} e\{(1)ik\}\right) \tag{29}$$

it is readily verified that the corresponding form for I is obtained by writing

$$-\frac{\mathrm{i}}{\omega}\int_0^\infty \varphi_1(q,\xi)\{1-\exp(-\mathrm{i}\omega\xi)\}\,\mathrm{d}\xi$$
$$= [\eta_0\{1-\omega^2\lambda_1\lambda_2) + 3\mu_0\eta_0\lambda_2 q^2 - 2\mu_0\lambda_1\sigma_0 q + \mathrm{i}\{\eta_0\omega(\lambda_1+\lambda_2) + \omega\lambda_1(\mu_0\eta_0\lambda_2 q^2$$
$$-\mu_0\sigma_0\lambda_1 q)\}]/(1-\omega^2\lambda_1{}^2 + \mu_0\lambda_1 q^2 + 2\mathrm{i}\omega\lambda_1) \tag{30}$$

$$\int_0^\infty\int_0^\infty \varphi_2(q,\xi_1,\xi_2)\{1-\exp(-\mathrm{i}\omega\xi_1)\}\{1-\exp(\mathrm{i}\omega\xi_2)\}\,\mathrm{d}\xi_1\,\mathrm{d}\xi_2$$
$$= \omega^2\eta_0\mu_0 q(\lambda_2-\lambda_1)(3-\mu_0\lambda_1 q^2 + 2\mathrm{i}\omega\lambda_1)/\{(1+\mu_0\lambda_1 q^2 - \omega^2\lambda_1{}^2 + 2\mathrm{i}\omega\lambda_1)$$
$$\times(1+\mu_0\lambda_1 q^2)^2\}. \tag{31}$$

From (23) and (27), it is seen that the unperturbed shear stress σ_0 and its derivatives with respect to the shear rate q are likely to be important when a steady shear and a small-amplitude oscillatory shear are superimposed. In figure 1 we have plotted typical curves of σ_0, $\mathrm{d}\sigma_0/\mathrm{d}q$ and $\mathrm{d}^2\sigma_0/\mathrm{d}q^2$ for the Oldroyd model (29).

Figure 2 contains theoretical (I, ω) curves for small values of q and realistic values of η_0, λ_1, λ_2 and μ_0. Figure 3 contains the corresponding (I, q) curves for various values of ω. The predicted shape of the curves for higher values of q is demonstrated in figures 4 and 5. The values of ϵ used in the computation were 0·0265 and 0·007. It will be observed that, even for these small values, quite large changes in the mean couple are predicted under some conditions.

† p_{ik} is the stress tensor, p an arbitrary isotropic pressure, $e_{ik}{}^{(1)}$ the rate of strain tensor and $\mathfrak{d}/\mathfrak{d}t$ is the convected time derivative introduced by Oldroyd (1950). η_0, λ_1, λ_2 and μ_0 are material constants. The usual tensor notation is implied.

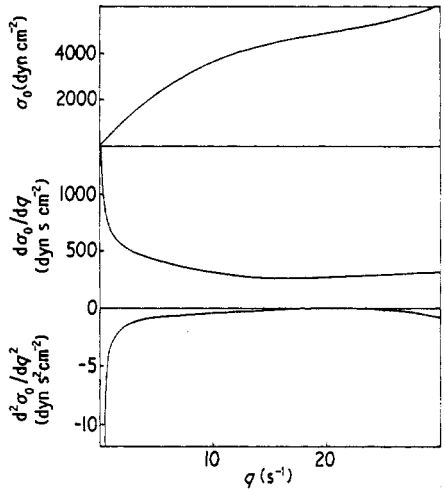

Figure 1. Curves of σ_0, $d\sigma_0/dq$, $d^2\sigma_0/dq^2$ for the Oldroyd model. $\eta_0 = 500$, $\lambda_1 = 1{\cdot}0$, $\lambda_2 = 0{\cdot}6$, $\mu_0 = 0{\cdot}01$.

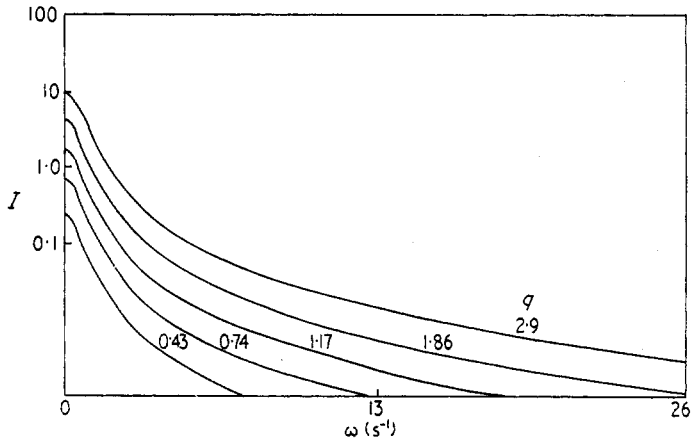

Figure 2. (I, ω) curves for $\eta_0 = 500$, $\lambda_1 = 1{\cdot}0$, $\lambda_2 = 0{\cdot}1$, $\mu_0 = 0{\cdot}01$, $\epsilon = 0{\cdot}0265$. Experimental conditions correspond to those of figure 7.

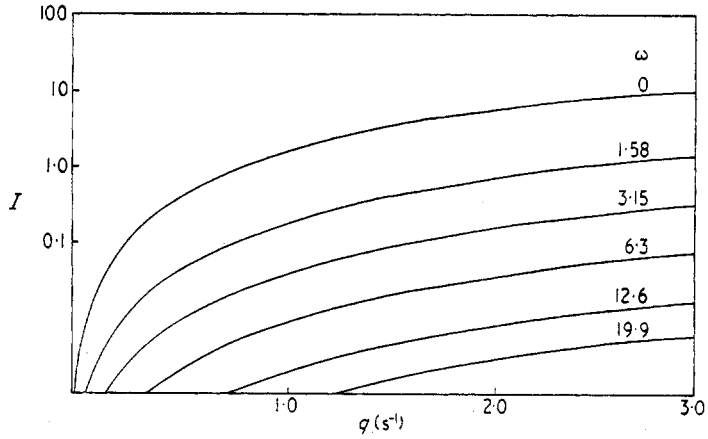

Figure 3. (I, q) curves for $\eta_0 = 500$, $\lambda_1 = 1{\cdot}0$, $\lambda_2 = 0{\cdot}1$, $\mu_0 = 0{\cdot}01$, $\epsilon = 0{\cdot}0265$. Experimental conditions correspond to those of figure 7.

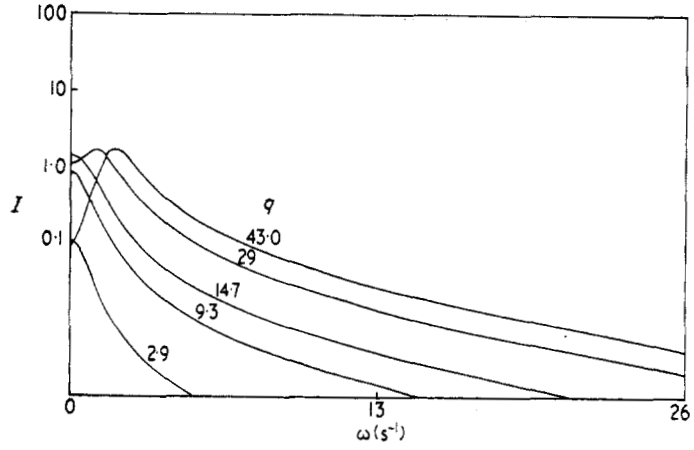

Figure 4. (I, ω) curves for $\eta_0 = 700$, $\lambda_1 = 1{\cdot}0$, $\lambda_2 = 0{\cdot}15$, $\mu_0 = 0{\cdot}0015$, $\epsilon = 0{\cdot}007$. Experimental conditions correspond to those of figure 7.

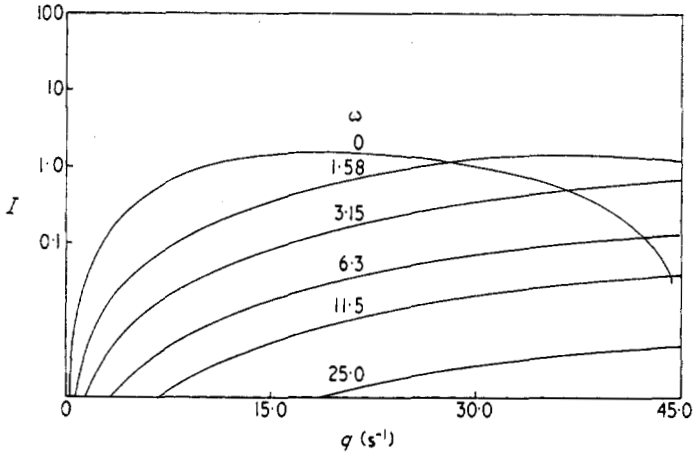

Figure 5. (I, q) curves for $\eta_0 = 700$, $\lambda_1 = 1{\cdot}0$, $\lambda_2 = 0{\cdot}15$, $\mu_0 = 0{\cdot}0015$, $\epsilon = 0{\cdot}007$. Experimental conditions correspond to those of figure 7.

3. Experimental results

The experimental results were obtained from a Weissenberg rheogoniometer model R16 manufactured by Sangamo Controls Ltd. With two drive-units available, a superimposed steady and oscillatory shear was readily available, and existing experimental techniques for uncoupled (steady or oscillatory) shear could be easily adapted to study the effect of the steady shear on the dynamic properties and also the effect of the oscillatory shear on the mean couple.

3.1. *Effects of steady shear on the complex viscosity*

In practice, the complex viscosity η^* is determined by measuring the amplitude ratio $\mathscr{I}$ of the motions of the cone and the plate and the phase lag c between them (cf. equation (5)). In the absence of fluid inertia, the equations for η' and G' are

(Walters and Kemp 1968, Walters 1968)

$$\eta' = \frac{-T\omega\mathscr{J}\sin c}{\mathscr{J}^2 - 2\mathscr{J}\cos c + 1} \tag{32}$$

$$G' = \frac{T\omega^2\mathscr{J}(\cos c - \mathscr{J})}{\mathscr{J}^2 - 2\mathscr{J}\cos c + 1} \tag{33}$$

where

$$T = \frac{3\theta_0}{2\pi a^3}\left(\frac{K}{\omega^2} - I\right). \tag{34}$$

K is the restoring constant of the torsion wire, I the moment of inertia of the cone about its axis, a the radius of the cone and θ_0 is the gap angle. Equations (32) and (33) were used in the present investigation to determine η' and G' as functions of frequency in the case of non-zero values of q.

A number of combined steady and oscillatory shear experiments were performed on various aqueous solutions of polyacrylamide.† The σ_0, $d\sigma_0/dq$ and $d^2\sigma_0/dq^2$

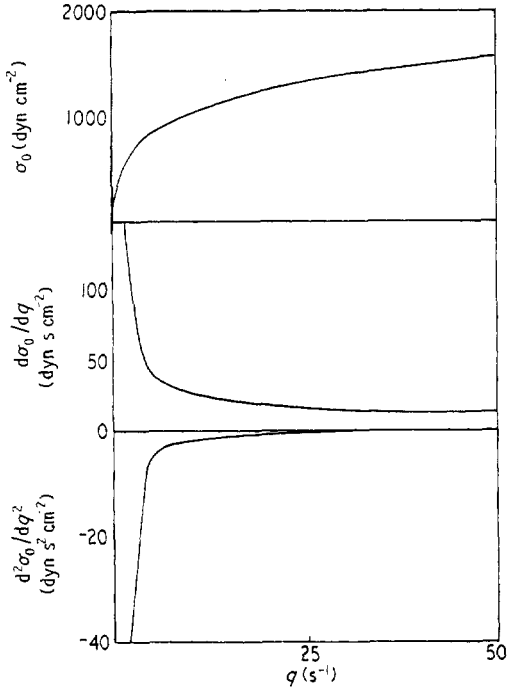

Figure 6. Experimental curves of σ_0, $d\sigma_0/dq$, $d^2\sigma_0/dq^2$ for a 5% aqueous solution of polyacrylamide.

curves for a 5% solution, which are typical of those obtained in the present investigation, are given in figure 6. It will be observed that the theoretical curves for the Oldroyd model (figure 1) show the same essential features as the experimental curves.

† Polyacrylamide P250 manufactured by Cyanamid of Great Britain.

Figures 7 and 8 contain (η', ω) and (G', ω) curves for various values of q for the 5% solution. We see that η' decreases with increasing q at each frequency and that negative G' values are possible at the lower frequencies. The curves are similar to those given in a previous communication (Walters and Jones 1968).

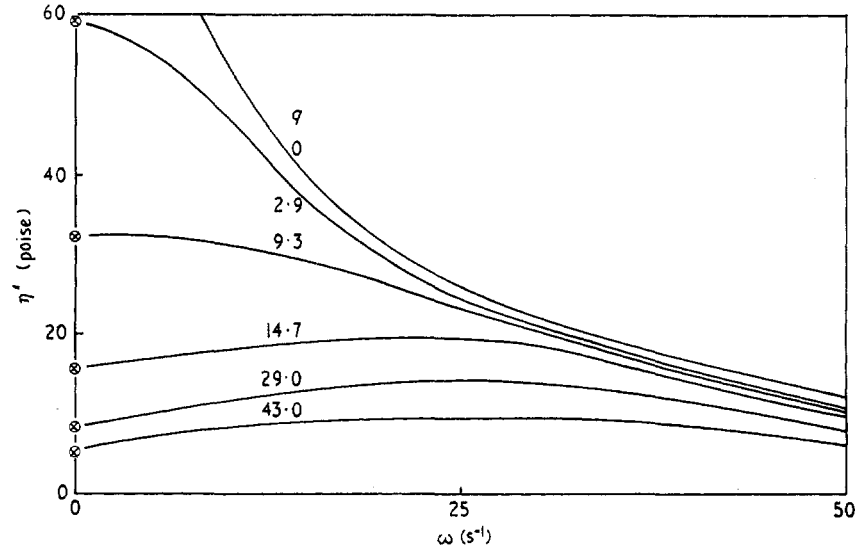

Figure 7. Experimental (η', ω) curves for a 5% aqueous solution of polyacrylamide. $K = 9{\cdot}034 \times 10^6$ dyn cm, $I = 1{\cdot}64 \times 10^3$ dyn cm s^2, $a = 3{\cdot}765$ cm, $\theta_0 = 1° 32'$. ⊗ theoretical prediction based on (24).

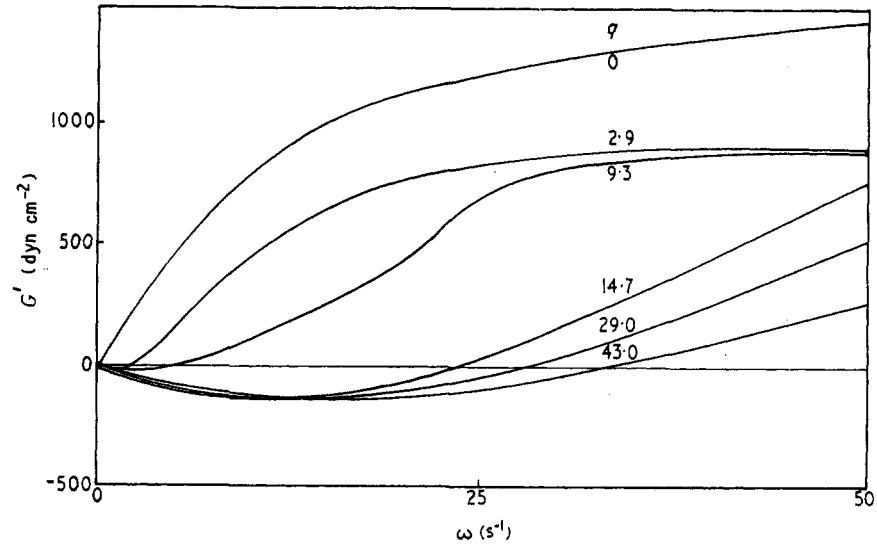

Figure 8. Experimental (G', ω) curves for a 5% aqueous solution.

Included in figure 7 are the $d\sigma_0/dq$ values obtained from figure 6. It will be observed that $\eta' \to d\sigma_0/dq$ and $G' \to 0$ as $\omega \to 0$ in agreement with the theoretical prediction (24).

Figure 9 and 10 contain complex viscosity data for a 4% solution and figures 11 and 12 the corresponding data for a 4·5% solution. The general features are the same as those for the 5% solution with prediction (24) valid in each case.

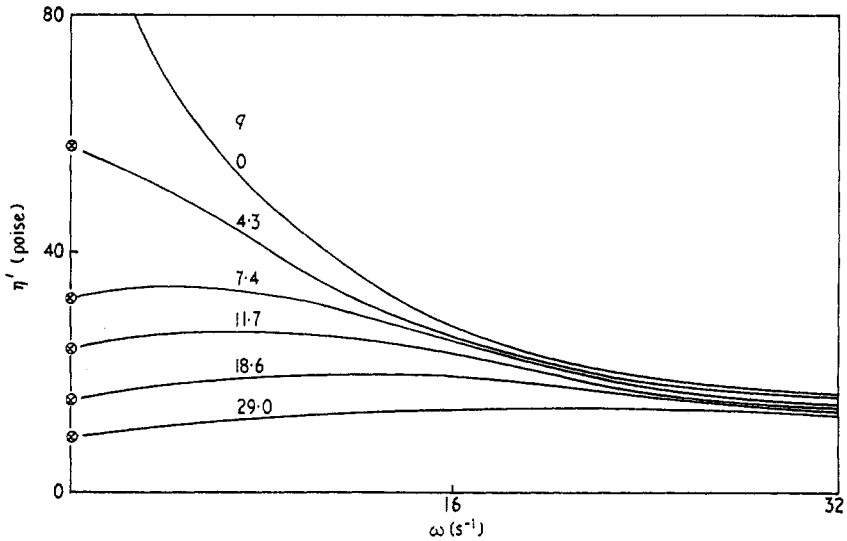

Figure 9. Experimental (η', ω) curves for a 4% solution of polyacrylamide. Experimental conditions as in figure 7. ⊗ theoretical predictions based on (24).

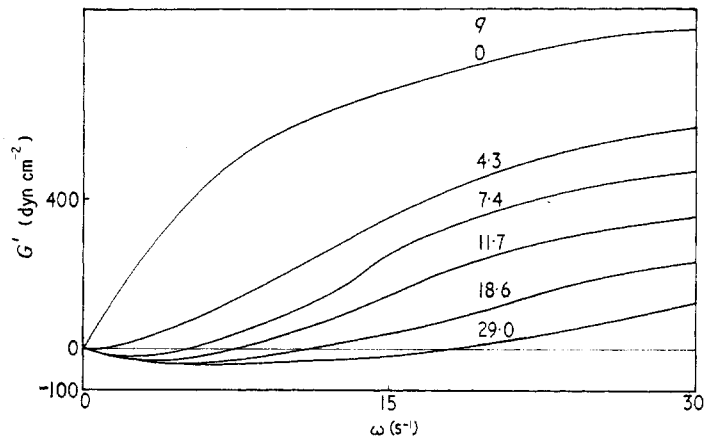

Figure 10. Experimental (G', ω) curves for a 4% solution of polyacrylamide.

In his experimental study of the same problem, Booij (1966 b) noticed that $G' = 0$ at frequencies which were given to a good approximation by $\omega = q/2$. In our earlier study (Walters and Jones 1968) we also noticed this feature. The current experiments on more concentrated solutions indicate that the empirical relation given above is not valid universally.

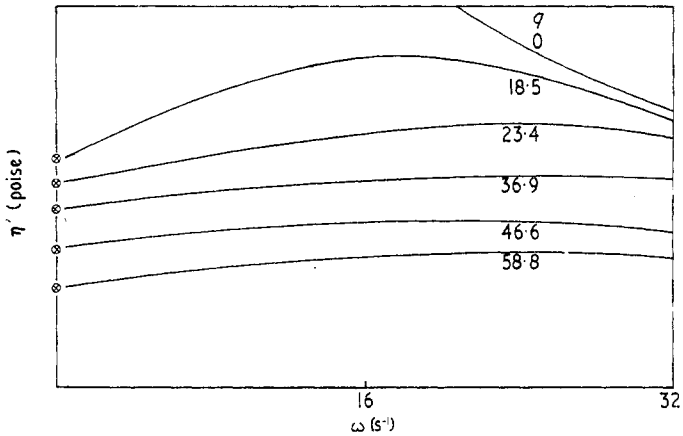

Fig. 11. Experimental (η', ω) curves for a 4·5% solution of polyacrylamide. Conditions the same as in figure 7. ⊗ theoretical predictions based on (24).

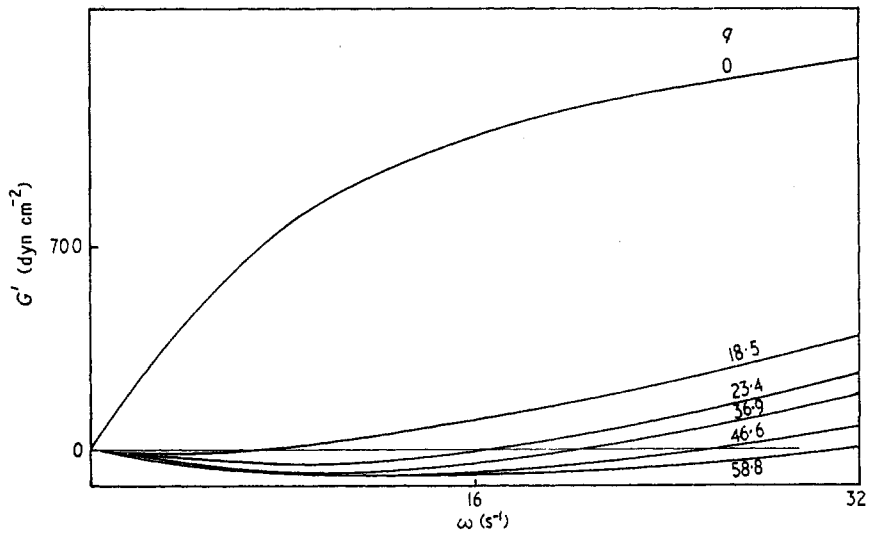

Figure 12. Experimental (G', ω) curves for a 4·5% solution of polyacrylamide.

3.2. *Effect of oscillatory shear on the mean shear*

We have indicated that combined steady and oscillatory shear experiments are very easily performed on the Weissenberg rheogoniometer. An investigation of the percentage change in the mean couple due to the oscillatory shear is particularly simple to carry out. The main limitation is caused by the relatively low value of the maximum amplitude of the oscillatory shear. This was 0·0285 radians in our case, so that we were limited to very low values of $\epsilon(= \alpha\omega/q)$ in cases of low frequencies or high shear rates. The small amplitude also means that any slight imperfection in the steady motion at high shear rates q can be of the same order of magnitude as the superimposed oscillatory shear. There is therefore a practical limitation on q.

Figure 13 contains curves of percentage decrease in couple I against frequency ω for various values of q and fixed α. It will be observed that $I \to 0$ as $\omega \to 0$ in agreement with the theoretical prediction of § 2. We remark, in passing, that figure 11 indicates a 30% decrease in mean couple for $\epsilon = 0{\cdot}2$.

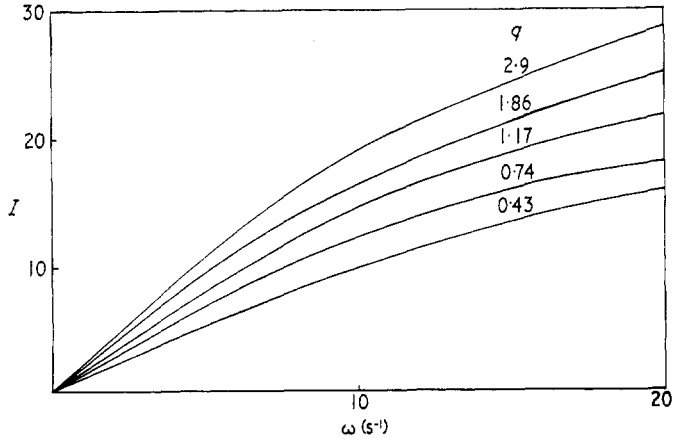

Figure 13. Experimental (I, ω) curves for fixed α (0·0285 rad) for a 5% aqueous solution of polyacrylamide.

The dependence of I on ϵ is illustrated in figure 14 for various values of ω and fixed q. It is clear that there is a substantial range of ϵ for which I is proportional to ϵ^2, in accordance with the theoretical result (26). At higher values of ϵ the curves

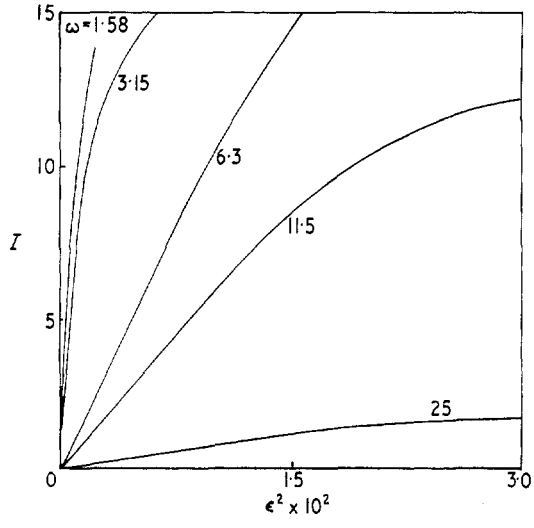

Figure 14. Experimental (I, ϵ) curves for fixed q (2·94 s^{-1}) for a 5% aqueous solution of polyacrylamide.

of I against ϵ^2 depart from a straight line and here terms of order ϵ^4 can no longer be ignored. All later experiments were performed within the region where I is proportional to ϵ^2, to enable a check to be made between theory and experiment.

Figures 15 and 16 illustrate, for a 4·0% aqueous solution of polyacrylamide, how I varies with ω for various values of q and with q for various values of ω. In each case $\epsilon = 0{\cdot}0283$. It is clear that the experimental curves have the same general shape as the theoretical curves based on the Oldroyd model (cf. figures 2 and 3). The comparable work of Booij (1966 a,b) on the influence of q on η^* would deter one from seeking a *quantitative* comparison between theory and experiment for such a simple fluid model.

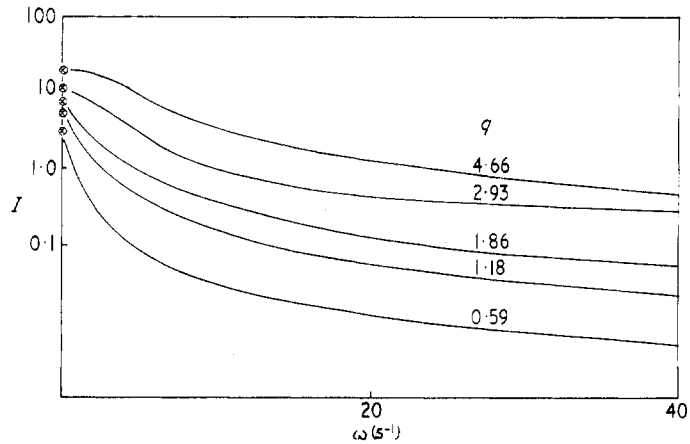

Figure 15. (I, ω) curves for a 4% solution of polyacrylamide. $\epsilon = 0{\cdot}0283$. ⊗ theoretical predictions based on (27).

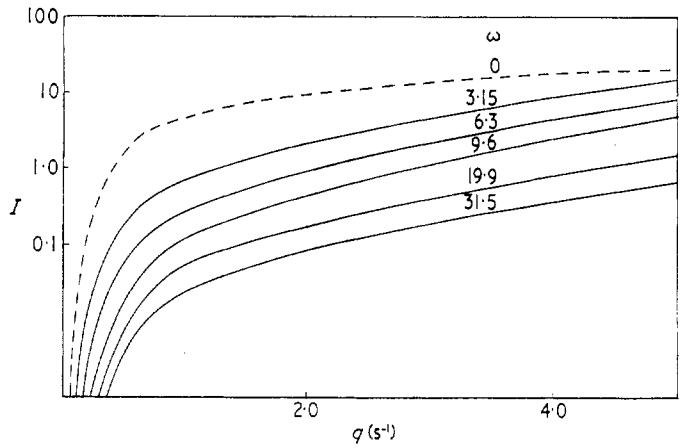

Figure 16. (I, q) curves for a 4% aqueous solution of polyacrylamide. $\epsilon = 0{\cdot}0283$. Broken line: theoretical prediction based on (27).

From figures 15 and 16 it is clear that I tends to non-zero values as ω tends to zero for fixed ϵ, in contrast with the situation in figure 13 where α was fixed in the limiting process.

Included in figures 15 and 16 are the theoretical values of I based on the 'inelastic' equation (27). It is clear that the experiments provide adequate confirmation of the theoretical predictions (27).

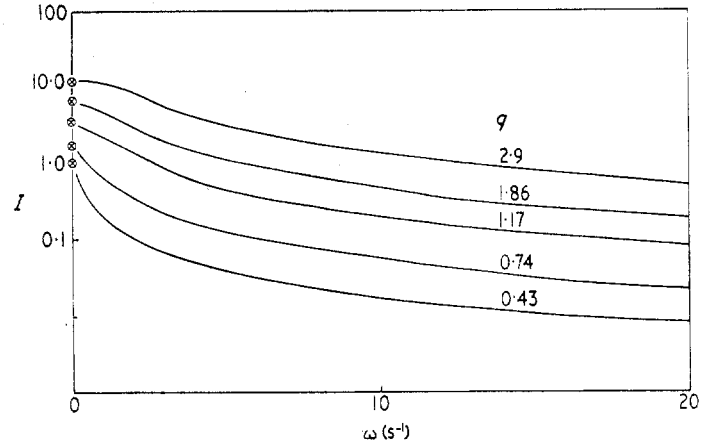

Figure 17. (I, ω) curves for a 4·5% aqueous solution of polyacrylamide. $\epsilon = 0{\cdot}0265$. ⊗ theoretical prediction based on (27).

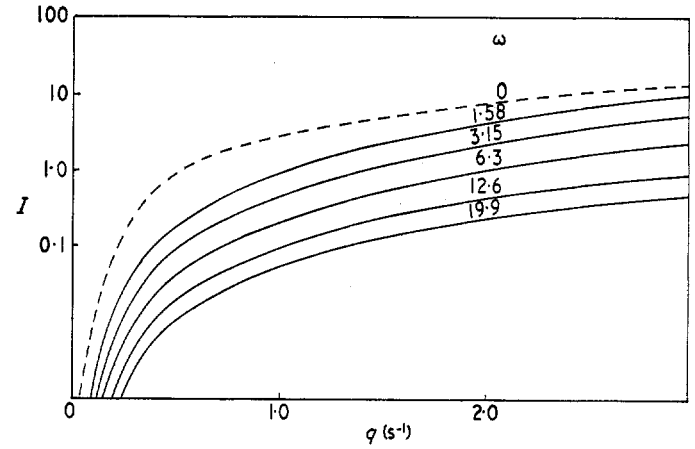

Figure 18. (I, q) curves for a 4·5% aqueous solution of polyacrylamide. $\epsilon = 0{\cdot}0265$. Broken line: theoretical prediction based on (27).

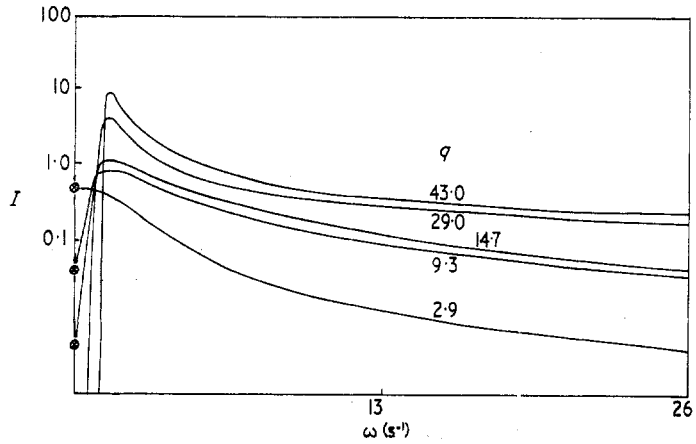

Figure 19. (I, ω) curves for a 5·0% aqueous solution of polyacrylamide. $\epsilon = 0{\cdot}007$. ⊗ theoretical prediction based on (27).

The various theoretical predictions, quantitative and qualitative, are further confirmed by figures 17 and 18 which contain results for a 4·5% aqueous solution of polyacrylamide.

In figures 19 and 20 for a 5% solution, we have taken relatively high values of q to illustrate the experimental results in this range. In this case, it is not possible to adequately check the inelastic prediction (27) on account of the experimental limitation on the amplitude of the oscillatory motion.

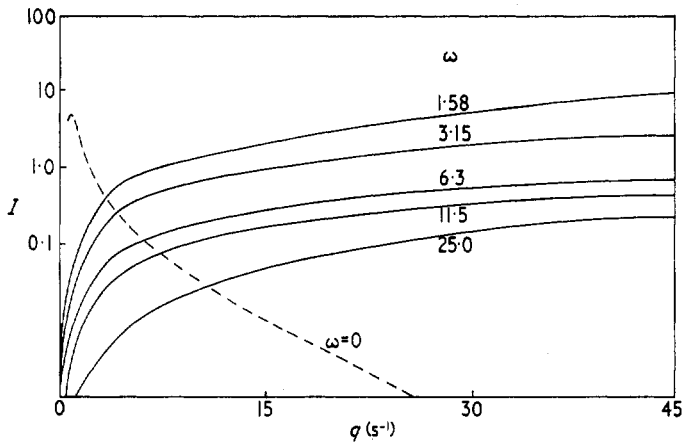

Figure 20. (I, q) curves for a 5·0% aqueous solution of polyacrylamide. Broken line: theoretical prediction based on (27).

4. Conclusions

On *theoretical* grounds, the fact that the relation between stress and shear rate is nonlinear in the case of elastico–viscous liquids immediately suggests that a superimposed oscillation on a steady shear should affect the mean stress. There have also been superficial attempts to investigate such an effect *experimentally*. However, we know of no detailed investigation, theoretical or experimental, of the sort given in the present paper. The work indicates that the experimental determination of the mean stress in the case of superimposed steady and oscillatory shear, which is very easy to perform in practice, would be a useful addition to the experiments which are already available for elastico–viscous model fitting.

As an important indirect conclusion of the present work, we remark that in *steady* shear experiments involving elastico–viscous liquids, the fact that any variation from a state of steady shear may be very small is no guarantee that this variation will not have a measurable effect on the mean conditions.

Acknowledgments

We are grateful to Sangamo Controls Ltd. for the loan of a drive unit.

References

Booij, H. C., 1966 a, *Rheol. Acta*, **5**, 215.

—— 1966 b, *Rheol. Acta*, **5**, 222.

Macdonald, I. F., and Bird, R. B., 1966, *J. phys. Chem.*, **70**, 2068.

Markovitz, H., 1968, in *Proc. 5th Int. Congr. on Rheology, Kyoto*, Vol. 1 (University Park Press), p. 499.

OLDROYD, J. G., 1950, *Proc. R. Soc.* A, **200,** 523.
—— 1958, *Proc. R. Soc.* A, **245,** 278.
OSAKI, K., TAMURA, M., KURATA, M., and KOTAKA, T., 1965, *J. phys. Chem.*, **69,** 4183.
PIPKIN, A. C., 1966, *Modern Developments in the Mechanics of Continua* (London: Academic Press), p. 89.
—— 1968, *Trans. Soc. Rheol.*, **12,** 397.
TANNER, R. I., 1968, *Trans. Soc. Rheol.*, **12,** 155.
TANNER, R. I., and SIMMONS, J. M., 1967, *Chem. Eng. Sci.*, **22,** 1079.
WALTERS, K., 1962, *Quart. J. Mech. Appl. Math.*, **15,** 63.
—— 1968, *Basic concepts and formulae for the Rheogoniometer* (Sangamo Controls Ltd.).
WALTERS, K., and JONES, T. E. R., 1968, in *Proc. 5th Int. Congr. on Rheology, Kyoto,* Vol. 4 (University Park Press).
WALTERS, K., and KEMP, R. A., 1968, *Polymer Systems—Deformation and Flow* (London: Macmillan), chap. 18.
WALTERS, K., and WATERS, N. D., 1968, *Polymer Systems—Deformation and Flow* (London: Macmillan), chap. 17.